

See discussions, stats, and author profiles for this publication at: <https://www.researchgate.net/publication/226662903>

The impact of glaciation, river–discharge and sea–level change on Late Quaternary environments in the southwestern Kara Sea

Article in *International Journal of Earth Sciences* · December 2000

DOI: 10.1007/s005310000119

CITATIONS

49

READS

81

6 authors, including:



Leonid Polyak

The Ohio State University

127 PUBLICATIONS 7,492 CITATIONS

[SEE PROFILE](#)



Mikhail Levitan

Russian Academy of Sciences

178 PUBLICATIONS 974 CITATIONS

[SEE PROFILE](#)



Tatyana. Abramovna Khusid

Russian Academy of Sciences

55 PUBLICATIONS 730 CITATIONS

[SEE PROFILE](#)

Some of the authors of this publication are also working on these related projects:



Pleistocene of the World Ocean continental margins [View project](#)



The stratigraphy of Quaternary ocean sediments and paleoceanology [View project](#)

Leonid Polyak · Mikhail Levitan · Valery Gataullin
Tatiana Khusid · Valery Mikhailov
Valentina Mukhina

The impact of glaciation, river-discharge and sea-level change on Late Quaternary environments in the southwestern Kara Sea

Received: 1 October 1999 / Accepted: 15 May 2000 / Published online: 5 September 2000
© Springer-Verlag 2000

Abstract Sedimentary records from the southwestern Kara Sea were investigated to better understand the extent of the last glaciation on the Eurasian Arctic shelf, sea-level change, and history of the Ob' and Yenisey river discharge. Sediment-core and seismic-reflection data indicate that the Quaternary depositional sequence in the southwestern Kara Sea consists of glacial, glaciomarine, and marine sedimentary units. Glaciogenic sediments in the deep Novaya Zemlya Trough are presumably related to the Last Glacial Maximum (LGM), whereas further east they may represent an earlier glaciation. Thus, it is inferred that the southeastern margin of the LGM Barents-Kara ice sheet was contained in the southwestern Kara Sea east of the Novaya Zemlya Trough. Changes in mineralogical, foraminiferal, and stable-isotopic composition of sediment cores indicate that riverine discharge strongly influenced sedimentary and biotic environments in the study area during the Late Weichselian and early Holocene until ca. 9 ka, consistent with lowered sea levels. Subsequent proxy records reflect minor changes in the Holocene hydrographic regime, generally characterized by reduced riverine inputs.

Keywords Kara Sea · Late Quaternary · Glacial geology · Sedimentary environments · Arctic rivers

Introduction

The Kara Sea shelf (Fig. 1) has experienced profound environmental changes, including interactions between Quaternary ice sheets, Siberian river runoff, and sea-level oscillations. The Kara Sea receives almost half of the total Arctic Ocean runoff from two of the world's largest river systems, the Ob' and Yenisey rivers. Presently, low-salinity riverine water spreads over approximately half of the Kara Sea. With lower sea levels, this estuarine circulation may have extended towards the northern margin of the shelf, interacting with eastward-flowing Atlantic-derived water. Quaternary records from western Siberia indicate that dramatic changes in large-scale hydrological processes accompanied the recurrent formation of ice sheets in northern Eurasia (e.g., Arkhipov et al. 1986; Astakhov 1992); however, neither the timing and extent of glaciations in the Kara Sea region nor its paleo-hydrology during the Quaternary are well understood. One scenario implies that the shallow Kara Sea shelf was a major ice-sheet center during glacial periods, including the Last Glacial Maximum (LGM; e.g., Grosswald 1994). According to another scenario, the LGM ice was moving into the Kara Sea from the Barents Sea and/or Novaya Zemlya for an unknown extent (Forman et al. 1995, 1999; Svendsen et al. 1999). Clarifying the configuration of ice-sheet margins in the Kara Sea is needed to provide improved boundary conditions for estimates of Eurasian ice-sheet volumes and to better understand the history of the Ob' and Yenisey river drainage, including the proposed formation of gigantic proglacial lake systems (Arkhipov et al. 1995).

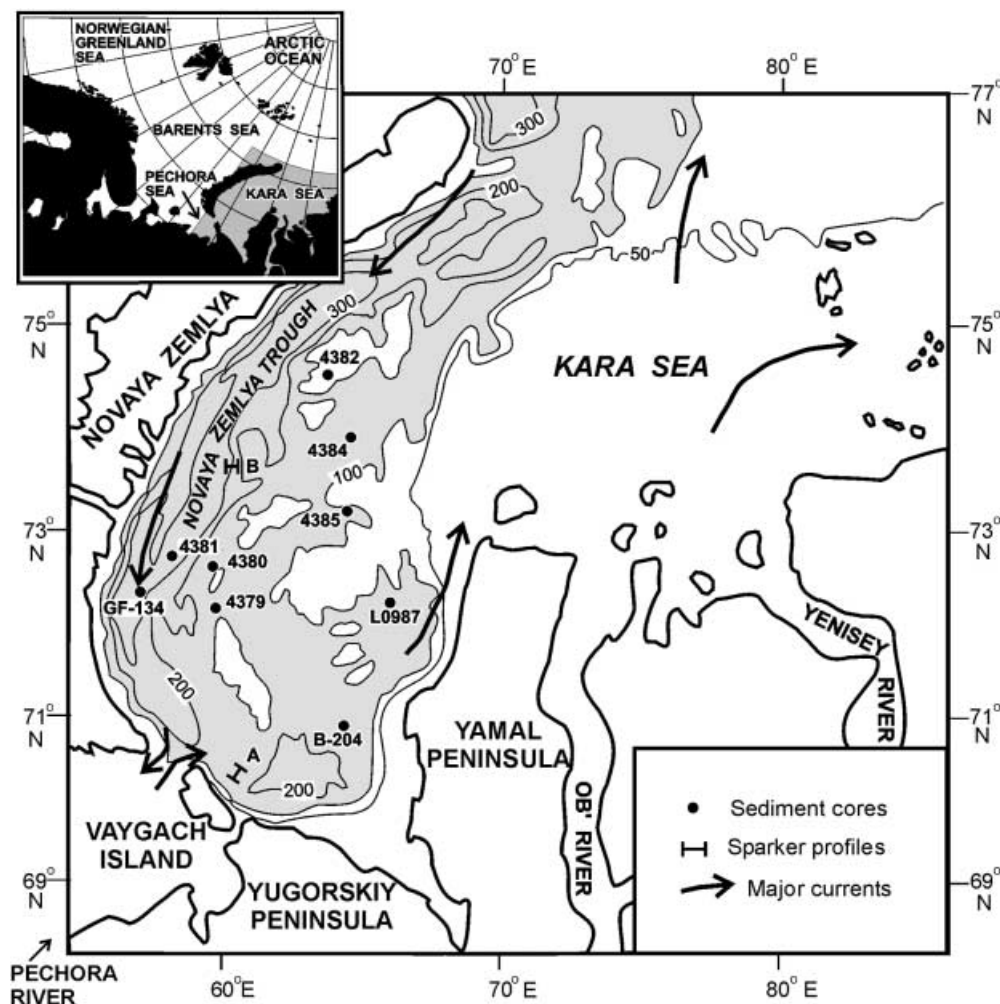
Seismic reflection records, sediment cores/boreholes, and coastal excavations indicate that Quaternary deposits in the Kara Sea reach up to 200 m in thickness, although their stratigraphic continuity and age are insufficiently understood (e.g., Valpeter et al.

L. Polyak (✉) · V. Gataullin
Byrd Polar Research Center, Ohio State University, Columbus,
OH 43210, USA
E-mail: Polyak.1@osu.edu
Phone: +1-614-2922602
Fax: +1-614-2924697

M. Levitan · T. Khusid · V. Mukhina
P.P. Shirshov Institute of Oceanology, 117218 Moscow, Russia

V. Gataullin · V. Mikhailov
Research Institute for Oil and Gas, LV-1226 Riga, Latvia

Fig. 1 Location map with bathymetry in 50, 100, 200, and 300-m contours; depths >100 m are shaded. Lettering is omitted in sediment core indexes for DM cores. Lines A and B show location of sparker records in Fig. 2A



1985; Gataullin 1992; Forman et al. 1999). Many sedimentary sequences have been disrupted by glacial activity and/or subaerial and shallow-marine processes. Favorable conditions for accumulation of Quaternary sediments occur in the relatively deep southwestern part of the Kara Sea bound by the islands of Novaya Zemlya and Vaygach on the west and by the Yamal Peninsula on the east (Fig. 1). Water depths in this region largely exceed 100 m and reach >500 m in the narrow Novaya Zemlya Trough. The southwestern Kara Sea has a wind-forced counterclockwise current pattern and is shaded by Yamal Peninsula from the direct impact of the Ob' and Yenisey river runoff (Pavlov and Pfirman 1995); however, during periods of higher discharge and/or lower sea levels, rivers likely affected the southwestern Kara Sea more profoundly. The shallow eastern part of this area has a homogenous water column; therefore, changes in riverine inputs are expected to have a direct effect on near-bottom water. The deep Novaya Zemlya Trough is likely to have a more complex response to river-induced changes, because it contains dense, fully saline bottom water produced by brines during the sea-ice formation.

We present seismic and sediment-core data from the southwestern Kara Sea, which aid understanding the LGM ice distribution and the postglacial development of sedimentary and hydrographic conditions in this area. Seismic reflection profiles and sediment cores, including ^{14}C age-controlled records, have been studied to establish the stratigraphy of the Quaternary sedimentary sequence. Special attention was given to analysis of heavy minerals as indicators of sediment sources and to foraminiferal assemblages and stable-isotopic composition of foraminiferal calcite, which reflect sea-bottom environments. The integration of these proxy data provides insights into the interplay between shelf-based glaciation, river discharge, sea level, and the thermohaline circulation in the Kara Sea.

Materials and methods

This study is based on materials that have been collected during several expeditions by the Institute of Oceanology of the Russian Academy of Sciences (IO-RAN), Research Institute for Marine Geology and

Table 1 Accelerator mass spectrometer ^{14}C ages

Lab no.	Core no.	Depth in core (m)	Material	Uncorrected age (years B.P.)
AA 34311	L0987	0.20–0.25	M* – detritus	2195±45
AA 14597	L0987	0.35–0.4	F – mixed	2819±46
AA 27910	L0987	0.65–0.7	M – <i>Yoldiella</i>	2835±60
AA 16836	L0987	1.1–1.15	F – mixed	6165±85
AA 16837	L0987	1.55–1.6	F – <i>E. bartletti</i>	8255±70
AA 27909	L0987	1.8–1.85	F – mixed	9685±70
AA 13021	L0987	2.1–2.15	F – <i>E. bartletti</i>	10200±85
AA 20483	GF-134	0.4	F – mixed	1825±105
AA 16838	GF-134	1.1	F – <i>Cornuspira</i>	3655±60
AA 20484	GF-134	2.47	F – mixed	9470±130
AA 27907	B-204	1.5–1.6	M – <i>Yoldiella</i> , <i>Thyasira</i>	1110±40
AA 27906	B-204	7.3–7.4	M – <i>Yoldiella</i>	1615±45
AA 27908	B-204	12.9–13.0	M – detritus	10145±70
PL9802346A	DM-4380	2.0–2.05	F – mixed	12170±100

Accelerator mass spectrometer laboratories: AA Arizona AMS Facility; PL Purdue University Laboratory; *M mollusks; F benthic foraminifers

Geophysics (NII Morgeo), Research Institute for Ocean Geology (Okeangeologia), Polar Marine Geological Expedition (PMGE), Arctic Marine Geotechnical Expedition (AMIGE), and Byrd Polar Research Center (BPRC) during 1984–1993 (Fig. 1; Valpeter et al. 1985; Gataullin et al. 1992; Lisitzin and Vinogradov 1995). Seismic reflection data were collected by NII-Morgeo/AMIGE for geotechnical studies and include sparker profiles run at frequencies of 200–1300 Hz and a source energy of 1.3 kJ (Valpeter et al. 1985). High-resolution acoustic penetration records were obtained by Okeangeologia/PMGE with a 5.5-kHz echo-sounder. Sediments were mostly recovered by gravity corers: L0987 (NII Morgeo 1984); DM-4379-4385 (R/V Dmitri Mendeleev 1993); and GF-134 (R/V Geolog Fersman 1993). We have also used samples from a borehole, B-204, drilled for geotechnical studies (Gataullin et al. 1992). Most sediment cores were described and logged for magnetic susceptibility on board ship and sampled for further investigation; GF-134 was preserved in a PVC liner prior to sampling. Cores were sampled at 5- to 20-cm increments and investigated for bulk density, water contents, grain size, and mineral and fossil composition. Initial results were previously reported for L0987 (Spesivtsev et al. 1986), B-204 (Gataullin et al. 1992), and DM cores (Levitan et al. 1995; Dunaev et al. 1996; Mukhina and Yushina 1999). We have reevaluated these data and performed additional investigation of heavy minerals, foraminifers, stable isotopes, and ^{14}C ages of selected cores to better understand Late Quaternary development of the southwestern Kara Sea. Age constraints were established using AMS ^{14}C dating of mollusk or foraminiferal calcite (Table 1). Heavy minerals were counted in a fine-sand fraction (50–100 μm in DM-93 cores and 63–106 μm in GF-134 and L0987) under a polarization microscope after separation at a density of 2.8 g/cm^3 . Foraminifers were counted in a >100- or >106- μm size fraction. Only calcareous foraminifers were used for interpretation due

to poor preservation of agglutinated tests. Most densely sampled cores GF-134 and L0987 were chosen for analysis of calcite stable isotopes in benthic foraminifer *Elphidium excavatum* f. *clavata*, which is a very common species in Quaternary sediments of the Arctic seas thriving in both full-marine and river-proximal environments (e.g., Hald et al. 1994). Although *E. excavatum* $\delta^{18}\text{O}$ is likely to be in disequilibrium with ambient water (McCorkle et al. 1990), its relative down-core changes allow us to characterize variations in water $\delta^{18}\text{O}$ composition. Determinations of $\delta^{18}\text{O}$ and $\delta^{13}\text{C}$ were performed on a Finnigan 252 MAT mass spectrometer at the Woods Hole Oceanographic Institution using standard procedures.

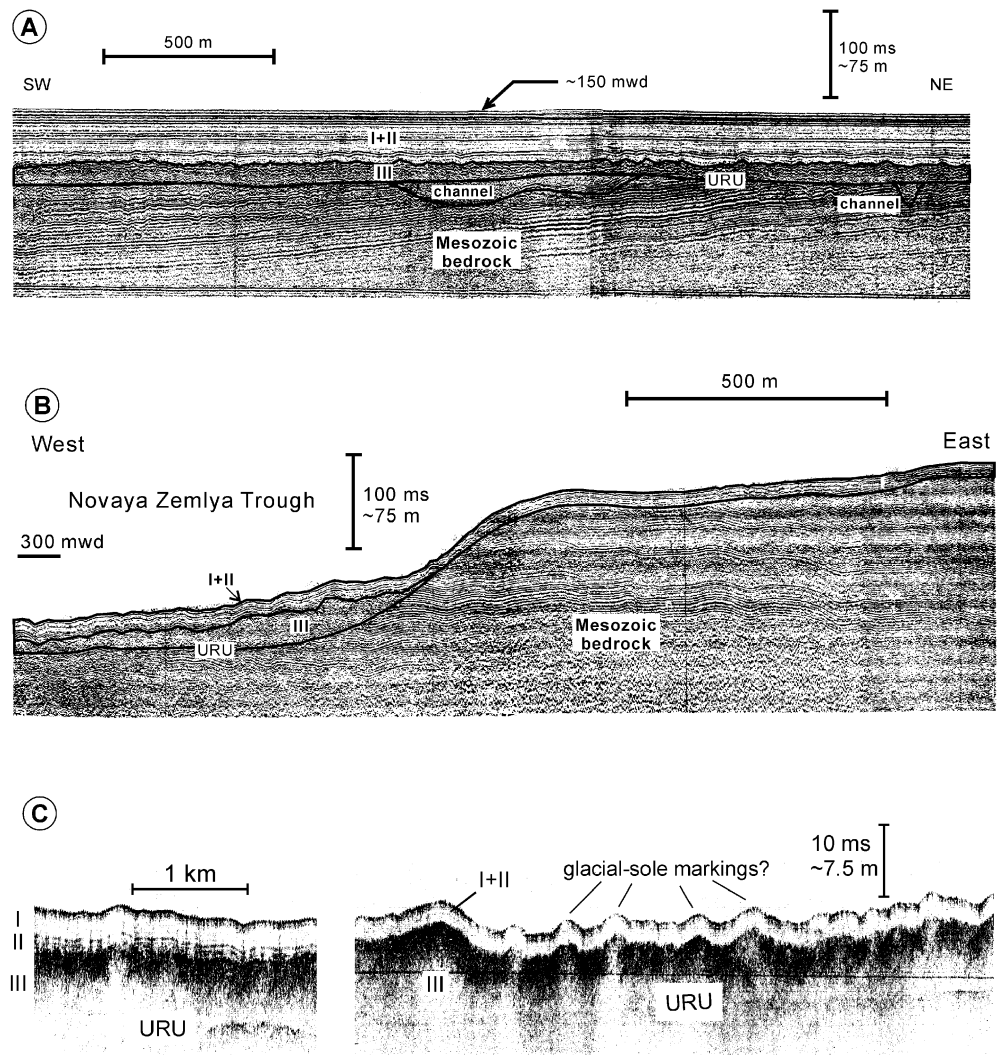
Results

Seismic stratigraphy

Interpretation and continuous tracing of seismic reflection records is often complicated in the Kara Sea by widespread gas- and/or ice-charged sediments (Valpeter et al. 1985). Accordingly, the seismic stratigraphy here is less clear and more fragmentary than in the Barents Sea (e.g., Solheim and Kristoffersen 1984). Below, we identify major seismic units for the study area, each characterized by its stratigraphic position, geometry, seismic signature, and appearance of top and bottom surfaces; however, additional study is required to provide a continuous regional correlation for these units.

Strata at the bottom of the sedimentary sequence penetrated by sparker records have strong, parallel, variably dipping reflectors, often sub-horizontally truncated at the top (Fig. 2). Borehole data from the Barents and Kara seas and geological data from adjacent mainland indicate that these strata are pre-Quaternary, and are mostly composed of soft Cretaceous or Paleogene sediments (Valpeter et al. 1985; Okulitch et

Fig. 2A–C Fragments of seismic reflection records exemplifying the structure of the Quaternary depositional sequence (Fig. 1 for locations). *I–III* glacial, glaciomarine, and marine sedimentary units, respectively; *URU* Upper Regional Unconformity. **A** Sparker record east of the Vaygach Island. **B** Sparker record across the eastern flank of Novaya Zemlya Trough. **C** 5.5 kHz echo-sounder records from Novaya Zemlya Trough (near cores GF-134 and DM-4381)



al. 1989). The truncation of these strata is correlated to the Upper Regional Unconformity (URU) which separates Quaternary from older deposits and can be traced over the Barents Sea shelf to its western margin (Solheim and Kristoffersen 1984; Sættem et al. 1992; Gataullin et al. 1993). In the sedimentary sequence above the URU, we identify three major seismic units, I–III, and correlate them to the seismic stratigraphy established for the southeastern Barents Sea (Krapivner et al. 1988; Gataullin et al. 1993; Gataullin et al., in press). A <50-m-thick unit occurs on top of the URU and has a chaotic seismic signature, variable thickness, and hummocky top surface. High-frequency acoustic records from the Novaya Zemlya Trough show that this surface is complicated by a system of low (2–5 m) ridges or hummocks which are reflected in the sea-floor topography (Fig. 2C). We identify this deposit as seismic unit III, shown in the Barents Sea to be a glacial diamicton (Gataullin et al. 1993; Gataullin et al., in press; Polyak et al. 1995). The bottom of unit III is sometimes complicated by

narrow incisions that are cut down to 25 m into bedrock (Fig. 2A). Similar incisions in the southern Barents Sea are interpreted as subglacial channels formed by erosional activity of ice or subglacial water (Gataullin and Polyak 1997). Unit III is conformably draped by a stratified sediment that generally increases in thickness southeastwards, reaching up to 50 m (Fig. 2A). This deposit is interpreted as a combination of postglacial seismic units I and II differentiated mostly on high-frequency acoustic records, which aid in distinguishing the stratified unit II from a more homogenous unit I (Fig. 2C).

Sediment stratigraphy and chronology

The sedimentary sequence penetrated by sediment cores can be subdivided into three major lithological units (Figs. 3, 4). This stratigraphy is based on sedimentary structures, physical properties of sediment [color, magnetic susceptibility (MS), water contents,

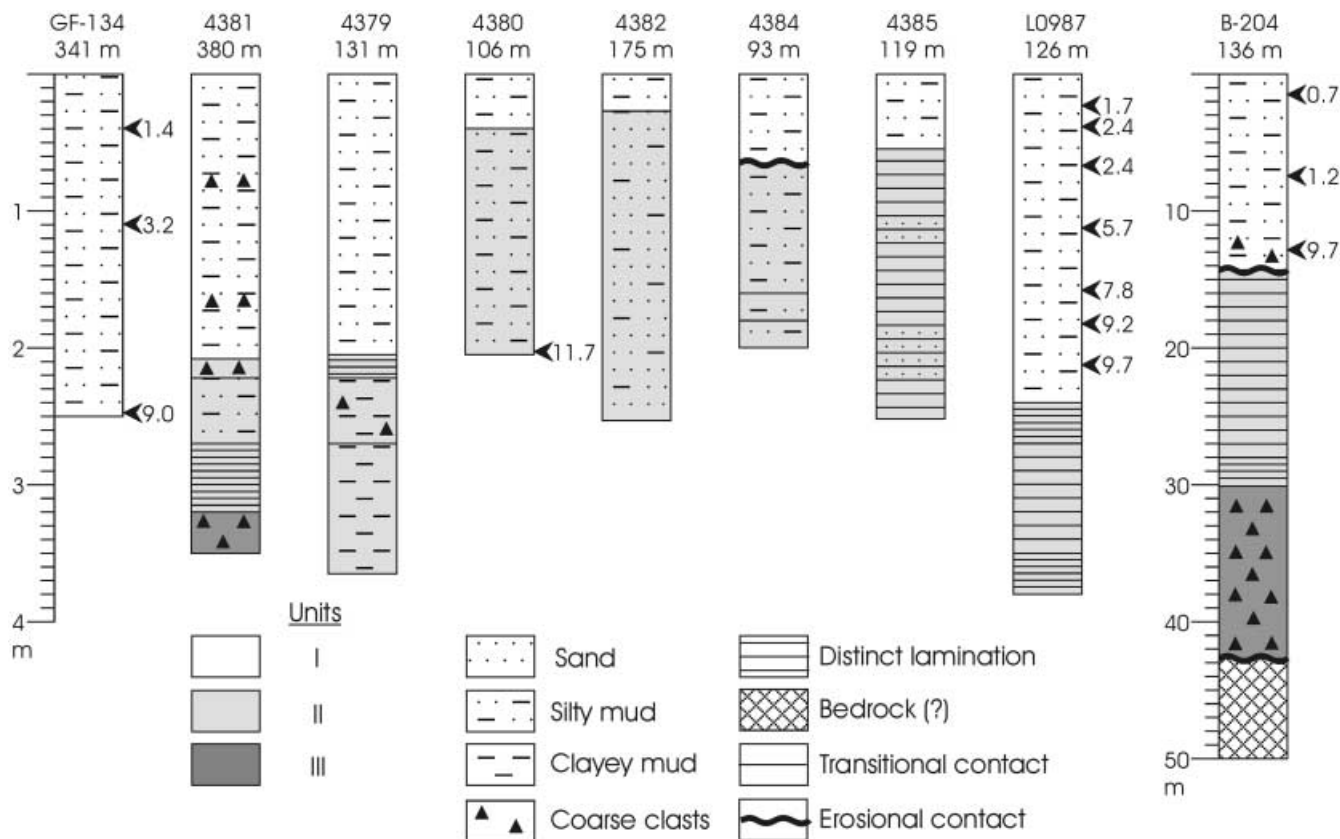


Fig. 3 Lithology of investigated sediment cores (Fig. 1 for locations). Water depth is shown under core numbers. ^{14}C ages (reservoir corrected) are shown to the right of the cores. Note change of depth scale for B-204

bulk density], grain-size contents, and mineralogical and microfossil composition.

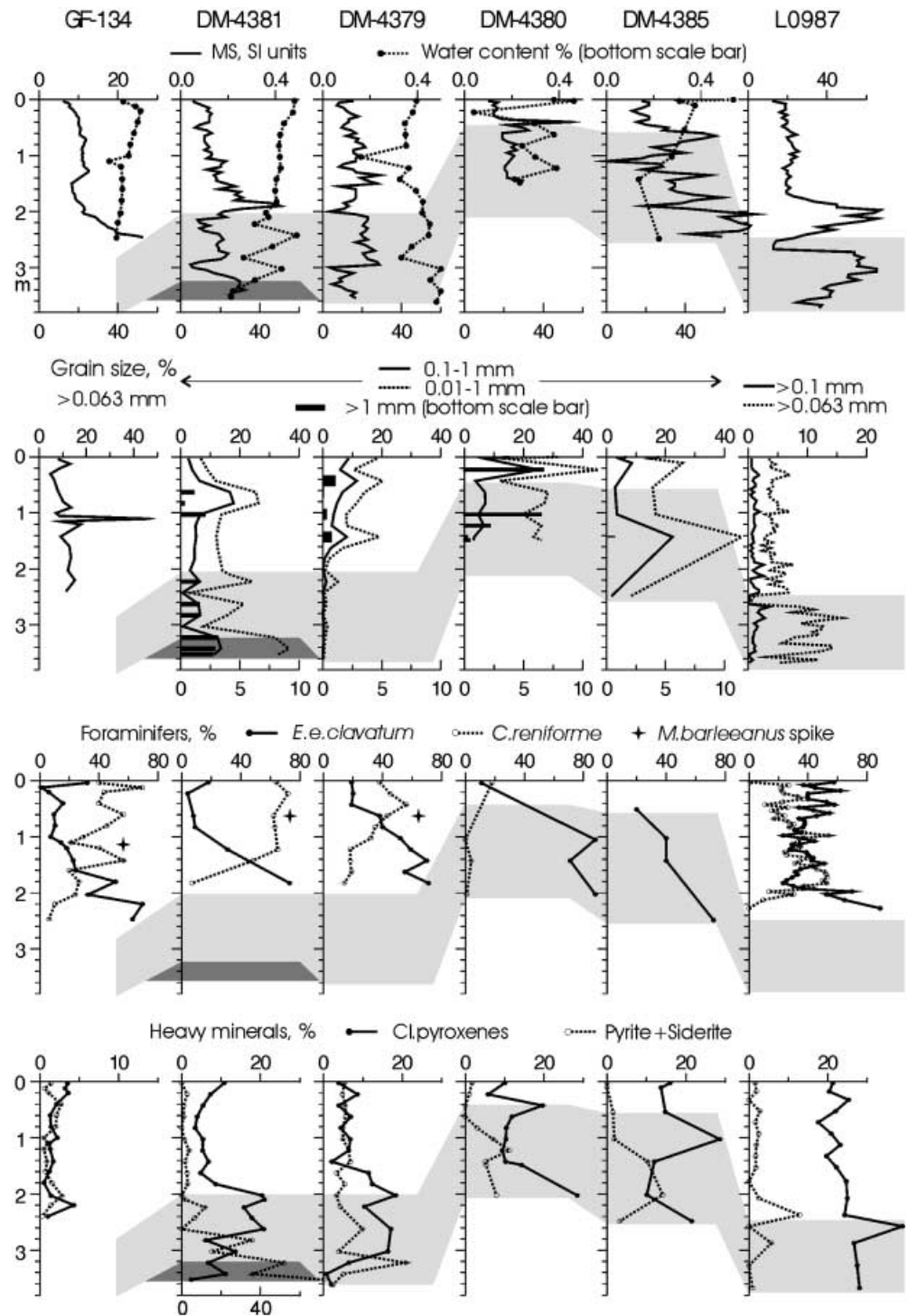
Sedimentary unit III was recovered in core DM-4381 from the Novaya Zemlya Trough and in several boreholes west of Yamal Peninsula, exemplified by B-204. This unit is a stiff, non-stratified, dark-gray diamicton with variable content of sand and coarser, typically subangular clasts (Fig. 5A). The erosional lower contact of unit III is demonstrated in B-204, where unit III lies on top of sand with unknown age (possibly bedrock) and contains detached lenses and bands of this sand. The diamicton is characterized by high bulk density ($>2 \text{ g/cm}^3$) and low water contents ($<30\%$). It completely lacks traces of biological activity but contains small numbers of microfossils, such as foraminifers that are often poorly preserved, and pre-Quaternary diatoms (Mukhina and Yushina 1999). Heavy-mineral associations of unit III are dominated by pyrite and detrital carbonates (mainly siderite).

Sedimentary unit II conformably overlies the stiff diamicton and is distinguished by a variable degree of lamination, gray to dark-gray or brownish coloration, relatively high water contents (mostly 30–50%), variable sand contents, elevated concentrations of clinopyroxenes, and almost complete absence of foraminifers

and other marine fossils (Figs. 3, 4, 5). Sediment lamination is caused by a cyclic alternation of clayey and silty laminae from a few millimeters to 1–2 cm thickness. Light-colored silty laminae have abrupt lower contacts and grade upwards into a darker clayey sediment with fine organic detritus. Lamination is distinct near the bottom of unit II in the Novaya Zemlya Trough (DM-4381) and throughout the whole unit in the eastern part of the study area. In core DM-4381, this unit contains two sandy layers similar in sediment properties and composition to the diamicton of unit III (Fig. 5A). The topmost stratigraphic level of unit II commonly has very low MS values, as exemplified in relatively high-resolution records DM-4381 and L0987. Additionally, in L0987 this level is distinguished by a fine lamination, very fine grain size, and an increased concentration of herbs in palynological spectra (Figs. 4, 5).

Sedimentary unit I is a soft (water content $>50\%$), olive-gray, bioturbated mud with numerous black iron-sulfide aggregates, polychaete tubes, and variable numbers of marine microfossils (e.g., calcareous and arenaceous foraminifers, ostracodes, small mollusks). Grain size as well as thickness of this sediment varies depending on the bathymetric position of core sites, with thinner and coarser sediments typical for the shallows. Sandy intervals also occur in cores from the Novaya Zemlya Trough. Mineralogical composition differs from the underlying sediments by having elevated concentrations of hornblende and/or garnets

Fig. 4 Major lithological, mineralogical, and paleontological characteristics of sediment cores along an approximate west–east transect across the study area (Fig. 1 for locations). *Light and dark gray shadings* highlight units II and III, respectively. Absolute MS values vary strongly between core sets due to different measuring procedures (whole cores vs isolated samples). Barite is added to pyrite+siderite values in DM-4379; *bottom scale bar* is used for pyrite+siderite in DM-4381



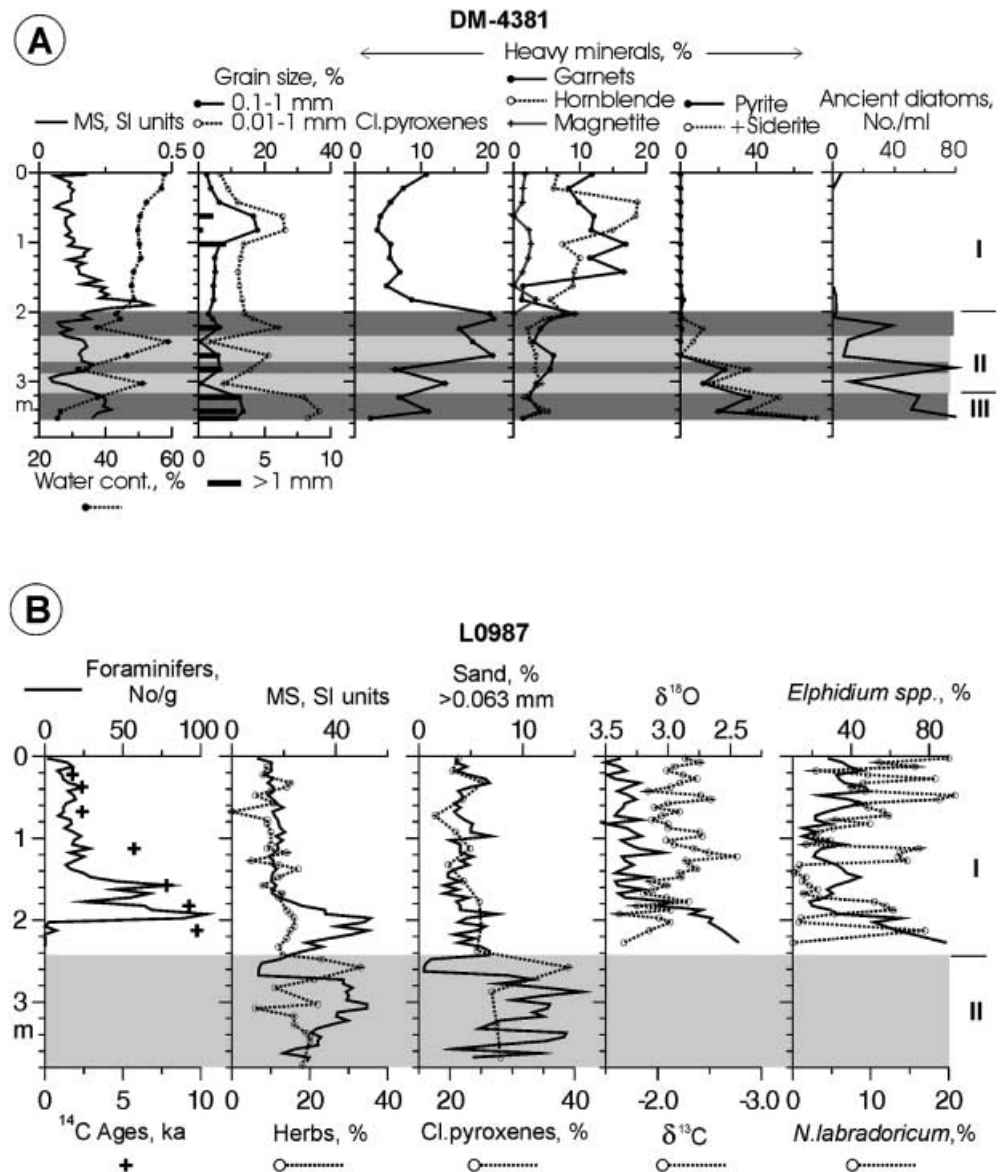
and the presence of fresh authigenic pyrite and magnetite (Fig. 5A). The MS values have a characteristic peak near the unit's bottom, as exemplified in DM-4381 and L0987. This unit mostly conformably overlies unit II, although in some cores from water depths <150 m, the boundary appears to be erosional.

A comparison of cores with acoustic penetration records, which can be exemplified by DM-4381 and a nearby acoustic record (Figs. 2C, 5A), indicates that

the three lithological units correspond to seismic units I–III. A similar correlation has been maintained for boreholes and sparker records (Valpeter et al.1985; Gataullin et al. 1992). We hereafter refer to the combined lithological and seismic units as sedimentary units I–III.

Age control was provided by AMS ^{14}C dates on mollusk shells or foraminifers picked from their abundance peaks in cores L0987, GF-134, DM-4380, and

Fig. 5 Detailed characterization of reference cores from the **A** western and **B** eastern parts of the study area. *Light and dark gray shadings* highlight units II and III, respectively. Intercalations of diamictic sediment in unit II in DM-4381 are shown as unit III (*dark gray*)



B-204 (Table 1). Most samples are from unit I and show Holocene ages (<10 ka). The only older date was obtained from unit-II sediment of DM-4380. We have used a standard oceanic reservoir correction of 400 years (Stuiver and Braziunas 1993). Age sequences in the dated cores show no inversions. There are two dates of 1.2 and 2.4 ka (B-204 and L0987, respectively) that appear to be too young in comparison with otherwise consistent age-depth patterns. These offsets could result from either increased sedimentation rates in the late Holocene, or from down-core transportation of analyzed shells. More detailed dating is required to elucidate the chronostratigraphic uncertainties.

Discussion

Depositional and paleo-ecological environments

Late Pleistocene

Lithological and seismic characteristics of sedimentary unit III are similar to those of glacial diamictos described from the Barents Sea and the Saint Anna Trough (e.g., Elverhøi and Solheim 1983; Sættem et al. 1992; Gataullin et al. 1993; Polyak et al. 1997a). The erosional lower boundary of unit III (Fig. 2), correlative to the URU of the Barents Sea, shows that the diamicton was associated with grounded ice overriding the shelf of the southwestern Kara Sea. Topographic features at the top surface of the diamicton in the Novaya Zemlya Trough (Fig. 2C) are similar in

size and shape to glacial-sole markings (flutes or transverse ridges) found on glaciated shelves including the Saint Anna Trough (Polyak et al. 1997a). The occurrence of these bedforms at a large water depth of almost 400 m is in line with their preferential preservation below the depth of iceberg keels that intensely scour seabed adjacent to a disintegrating ice sheet.

Diamictons from B-204 and other boreholes contain fragments (bands and blocks) of underlying strata, apparently detached from their bed (Valpeter et al. 1985; Gataullin et al. 1992). This type of sedimentary structure is common for the lower part of glacial diamictons in the Barents Sea and is attributed to a subglacial entrainment of the frozen or pressurized substratum (Sættem et al. 1992; Gataullin et al. 1993). We conclude that this process is also responsible for pyrite- and siderite-rich (>60%) heavy mineral composition of diamictons in the study area, as well as elsewhere in the Barents Sea and the Saint Anna Trough (Figs. 4, 5A; Yashin et al. 1985; Polyak and Solheim 1994; Polyak et al. 1997a). The in situ formation of these minerals in high amounts in glacial diamictons is not realistic. For a comparison, the contents of their authigenic forms in Holocene sediments do not exceed 5–10%. It is the pyrite- and siderite-rich Mesozoic sedimentary bedrock that is the main source for overlying deposits. Concentrations of pyrite and siderite strikingly co-vary with the numbers of pre-Quaternary diatoms (Fig. 5A), which further corroborates that these minerals have been redeposited. Considering that they are easily destroyed by transportation in water, high abundance of pyrite, and/or siderite in Quaternary sediments of the Barents and western Kara Sea can be used as an indicator of sub- or at least near-glacial environments.

Sedimentary unit II is heterogeneous and may include laminated and more homogenous facies, as well as diamictic intercalations. Lamination indicates a cyclic sediment delivery combined with absent or very low bioturbation. Cyclicity was possible due to seasonal or quasi-seasonal sediment inputs from coastal and/or sea-bottom erosion, riverine discharge, and glacier melting. All three causes could be significant for the study area during deglaciation and sea-level rise. Weak bioturbation was possibly associated with deglacial and/or low-sea-level settings due to decreased water salinities and strong turbidity, likely in combination with prolonged periods of sea-ice cover. We believe that laminated sediments occurring directly on top of glacial diamictons, such as in the Novaya Zemlya Trough (Figs. 2C, 5A), reflect near-glacial environments (cf. Lubinski et al. 1996; Polyak et al. 1997a), whereas thick laminated strata in the eastern part of the study area were potentially formed by coastal erosion and/or riverine inputs. Unit II from Novaya Zemlya Trough, exemplified by DM-4381, additionally contains two layers similar to glacial diamictons in having low water contents, elevated contents of sand and coarser clasts, and high concentrations of pyrite

and/or siderite and pre-Quaternary diatoms (Fig. 5A). Similar diamictic intercalations in the same stratigraphic position were found in the St. Anna Trough and interpreted as iceberg-rafted deposits (Polyak et al. 1997a). Intense iceberg rafting commonly accompanies marine deglacial environments, and the preservation of discrete iceberg-laden sedimentary layers is most likely to occur at large water depths where the sea floor is not turbated by icebergs.

Mineralogical associations of unit II are characterized by relatively high concentrations of clinopyroxenes, generally increasing eastwards to >30% in L0987 (Fig. 5B). Presently, clinopyroxenes in the Kara Sea originate mainly from the Siberian basaltic formations drained by the Yenisey river. An additional source for the northwestern part of the sea is provided by basaltic outcrops on Franz Josef Land (Kulikov 1971; Levitan et al. 1996; Behrends 1999). The eastward increase in pyroxene contents in the southwestern Kara Sea apparently reflects sediment delivery by Siberian rivers; thus, high pyroxene concentrations indicate that unit-II sedimentary environments were strongly affected by riverine inputs. This interpretation is corroborated by the composition of pore water in unit-II sediments that have concentrations of chlorine ion as low as <1 g/l in DM-4385 (Levitan et al. 1995). Down-core fluctuations in pyroxene contents may reflect variations in relative contributions of riverine sources vs glacial melting and/or coastal erosion.

A peak of clinopyroxenes commonly marks the uppermost part of unit II; in relatively high-resolution cores, such as DM-4381 and L0987, this peak co-occurs with low MS. In L0987 this stratigraphic level also coincides with fine lamination, very fine grain size, and a maximum of herbaceous pollen in palynological spectra (Fig. 5B). Sediments in a similar stratigraphic position from deeper areas in the Barents Sea and St. Anna Trough have pronounced interval of low MS. They are also characterized by a distinct oxidation indicative of very low sedimentation rates, confirmed by ^{14}C ages in some cores (Polyak et al. 1995, 1997a). We suggest that this stratigraphic level in the Kara Sea corresponds to a time of high riverine inputs combined with severe sea-ice cover, in turn associated with harsh climatic conditions. The herbaceous spike might attest to the Younger Dryas age that was reflected in cold and dry conditions along the Kara Sea coasts (Serebryanny et al. 1998; Hahne and Melles 1999). More palynological data from marine records are needed to test this assumption.

Holocene

The most distinctive feature of unit I is the abundant traces of biological activity: intense bioturbation; skeletal remnants of marine organisms; and iron-sulfide aggregates that replace decomposed organic tissues. These characteristics indicate that deposition of

unit I occurred in marine environments with relatively high biological productivity, generally similar to present conditions in seasonally ice-free Arctic seas and contrasting to glaciomarine and/or brackish-water and low-nutrient environments during the Late Weichselian. The bottom of unit I is marked by a peak in magnetic susceptibility that is typically well defined in cores with high resolution, such as DM-4381 and L0987, and can be traced over large distances into the St. Anna Trough and the Barents Sea (Polyak et al. 1997a). The wide geographic distribution and the consistency of the stratigraphic position of this peak at the bottom of iron-sulfide enriched sediment suggest that it is not controlled by magnetic properties of source rocks, but instead results from the in situ formation of magnetic minerals, such as pyrrhotite and greigite, at the initial stage of marine, biologically productive environments, which still had reduced salinities. A similar magnetization peak occurred in the Baltic Sea at the transition from varved sediment of the early Yoldia Sea to iron-sulfide-enriched sediment deposited in brackish water at ca. 10 ka (Sohlenius 1996).

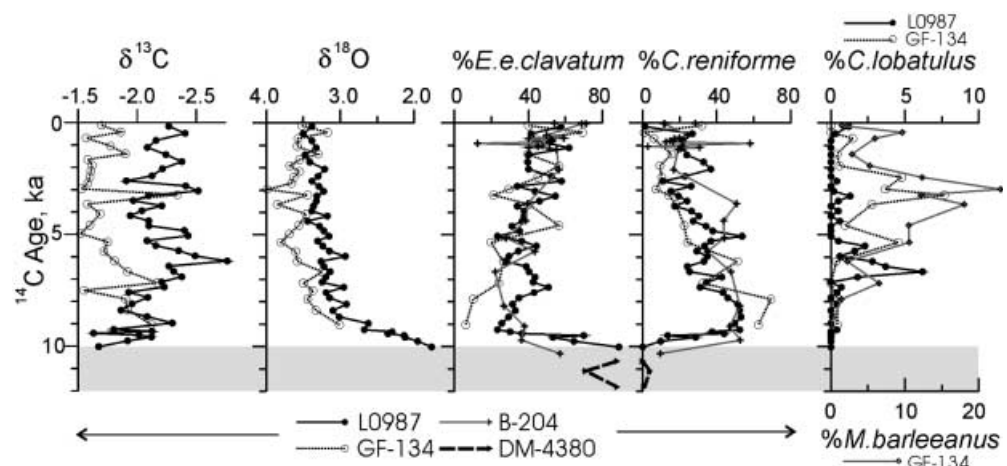
Changes in foraminiferal assemblages and stable isotopes from foraminiferal calcite in the lower part of unit I reflect the transition from brackish- to normal-marine environments that occurred between approximately 10 and 9 ka (Fig. 6). Benthic assemblages at the bottom of unit I are almost entirely composed of *Elphidiidae*, such as *Elphidium excavatum* f. *clavatum*, *E. incertum*, *E. bartletti*, and *Haynesina orbiculare*, which is typical for river-proximal Arctic environments (e.g., Hald et al. 1994; Khusid and Korsun 1996). This foraminiferal composition co-occurs with anomalously light calcite $\delta^{18}\text{O}$ values which are also indicative of riverine proximity on the Arctic shelves presently (Erlenkeuser et al. 1999). By 9 ka, $\delta^{18}\text{O}$ increased to values typical for the rest of the Holocene and *Elphidiidae* gave way to *Cassidulina reniforme* as a most abundant foraminiferal species. These changes indicate that at the beginning of the Holocene, the Ob' and Yenisey rivers were sufficiently

extended onto the Kara Sea shelf to affect its southwestern areas. By approximately 9 ka, the influence of rivers waned, reflecting their withdrawal toward present estuaries with postglacial sea-level rise (Fairbanks 1989).

Although subsequent variations in unit I are less pronounced, they include changes in foraminiferal assemblages, grain-size contents, and calcite stable-isotopic composition, especially $\delta^{13}\text{C}$ (Figs. 4, 5, 6). The $\delta^{18}\text{O}$ values show minor variability of 0.2–0.3 ‰, sometimes up to 0.5 ‰, which still exceeds the measurement inaccuracies and thus reflects changes in oceanographic conditions. $\delta^{13}\text{C}$ values show even more pronounced fluctuations of 0.5–0.8 ‰, mostly in phase with $\delta^{18}\text{O}$ variations, which is especially apparent in the Novaya Zemlya Trough (GF-134). Presently, both $\delta^{18}\text{O}$ and $\delta^{13}\text{C}$ contents in biogenic calcite in the Kara Sea are largely controlled by river runoff (Erlenkeuser et al. 1999), and we suggest that their co-variable excursions in the Holocene reflect variations in riverine inputs. Transfer of the stable-isotope signal downward from the surface of the water column via sea-ice brines can affect benthic stable-isotope values in the Novaya Zemlya Trough, possibly explaining larger-amplitude $\delta^{18}\text{O}$ variations in GF-134 than in L0987 (Fig. 6). The offset in stable-isotope values between the two cores after approximately 7 ka reaches 0.5‰ in $\delta^{18}\text{O}$ and almost 1‰ in $\delta^{13}\text{C}$. Judging from the southern Kara Sea data, these values may correspond to a salinity difference of several parts per million at the high-salinity end (Erlenkeuser et al. 1999). We suggest that this offset reflects the build-up of full-saline deep water in the Novaya Zemlya Trough and/or the weakening of riverine influence on the western part of the study area.

Benthic calcite $\delta^{13}\text{C}$ can be modified by remineralization of organic matter, thus reflecting biological productivity (e.g., McCorkle et al. 1990). This connection is corroborated for the study area by a co-variation in $\delta^{13}\text{C}$ record through most of L0987 with the content of benthic foraminifer *Nonion labradoricum* (Fig. 5B), which has an infaunal habitat and strongly depends on

Fig. 6 Stable-isotope (*E.e.clavatum*) and foraminiferal characterization of age-controlled sediment records plotted vs. ^{14}C age. $\delta^{18}\text{O}$ values are sea-level adjusted (Fairbanks 1989)



food fluxes to the sediment. Since biological productivity in the Kara Sea is largely associated with riverine nutrient inputs (e.g., Vedernikov et al. 1994), there are even more reasons to conclude that light $\delta^{13}\text{C}$ excursions reflect episodes of increased runoff. In contrast, heavy ^{13}C values occur in the early Holocene, before 9 ka, otherwise characterized by indications of elevated riverine discharge. This discrepancy might reflect very low-productivity environments prior to the establishment of fully interglacial conditions.

The stable-isotopic departure of GF-134 from L0987 at ca. 7 ka and a further $\delta^{18}\text{O}$ enrichment until ca. 3 ka in GF-134 co-occur with changes in foraminiferal assemblages, grain size, and mineralogy which indicates changes in water circulation patterns (Figs. 4, 5, 6). Foraminiferal species *Cibicides lobatulus* and *Melonis barleeanus* which are presently abundant in the study area only along the coast of Novaya Zemlya and at the adjacent flank of the trough, respectively (Polyak et al. 1997b), increase in abundance in cores L0987 and GF-134 after 7 ka and reach their maximum in the Novaya Zemlya Trough at around 3 ka (Figs. 4, 5, 6). This maximum coincides with a sandy layer with up to 50% sand and an admixture of coarser clasts. Heavy-mineral associations in the mid-Holocene interval of the Novaya Zemlya Trough cores are characterized by elevated contents of hornblende and garnets (Fig. 5A), suggesting that the Novaya Zemlya coasts and sea-floor shallows were major source areas (Kulikov 1971). We infer that the above changes reflect the intensification of a surface water circulation and/or the decrease in runoff, which limited riverine inputs to the eastern part of the southwestern Kara Sea between ca. 7 to 3 ka. Afterwards, this trend was presumably reverted, as indicated by lighter $\delta^{18}\text{O}$ values and a decrease in contents of sand, garnet/hornblende, and foraminifers *C. lobatulus* and *M. barleeanus* in the Novaya Zemlya Trough. As in the early Holocene, *Elphidiidae* became the most abundant foraminiferal group throughout the study area, reaching >50% in foraminiferal assemblages after ca. 3 ka. This was possibly related to an increase in riverine inputs and/or to heavier sea-ice conditions (cf. Hald et al. 1994; Polyak and Mikhailov 1996).

Glaciation limits

A widespread occurrence of glaciogenic sedimentary unit III in the southwestern Kara Sea shows that this region has been entirely covered by glacier ice at some time in the Quaternary. This scenario is consistent with the findings of glacial deposits and marginal features indicating the southward movement of ice sheets onto the western Siberian coastal plains, although the timing of these glacial events is debatable (e.g., Arkhipov et al. 1986; Astakhov 1992). Recent investigations employing modern chronostratigraphic techniques show that an ice sheet invaded the

Pechora Lowland and Yugorski and Yamal peninsulas from the Kara Sea in post-Eemian time, likely in the Early-Middle Weichselian, but not during the LGM (Mangerud et al. 1999; Forman et al. 1999; Lokrantz et al. 2000). These results fit data from the Pechora Sea indicating that the LGM ice did not extend into the southeastern sea area adjacent to the Pechora Lowland (Polyak et al., 2000; Gataullin et al., in press).

The occurrence of glaciogenic diamicton (unit III) beneath a thin cover of glaciomarine sediments in the Novaya Zemlya Trough (Figs. 2B,C, 5A) indicates that the trough was overrun by a grounded LGM ice sheet. Ridges or hummocks at the diamicton surface are similar to morphological features found on recently deglaciated continental shelves, such as flutes and transverse ridges (e.g., Solheim et al. 1990; Polyak et al. 1997a). The abrupt up-core decrease in the content of glacially reworked sediment constituents, such as pyrite/siderite grains and ancient diatoms (Fig. 5A), reflects the ice-margin retreat from the trough. This retreat was presumably punctuated by two episodes of accelerated iceberg calving marked by the diamictic intercalations in unit II in the deep part of the trough (DM-4381), similar to the St. Anna Trough (Polyak et al. 1997a). We consider the ^{14}C age of 11.8 ka from glaciomarine sediment in GF-4380 immediately east of the Novaya Zemlya Trough as a minimum age for deglaciation. Its completion is apparently marked by the establishment of interglacial conditions across the southwestern Kara Sea by ca. 10 ka (Figs. 3, 5, 6).

In contrast to the Novaya Zemlya Trough, the eastern part of the study area has an order-of-magnitude thicker unit II (up to 50 m; Figs. 2A, 3), which was possibly deposited for a much longer time. Although this deposit is not age-constrained below the Holocene, a comparison with the southeastern Pechora Sea (Polyak et al. 2000; Gataullin et al., in press) and with the coastal sections of the Yamal and Yugorski peninsulas (Forman et al. 1999; Lokrantz et al. 2000) suggests accumulation since the retreat of the Middle/Early Weichselian glaciation >40 ka; thus, the southeastern LGM limit is located east of the Novaya Zemlya Trough, roughly between 60° and 65°E (Fig. 7). We infer that heightened contents (10–20%) of glacially reworked mineral grains in unit-II sediment of cores DM-4380 to DM-4385 (Fig. 4) reflect the proximity of a glacier margin. This inference is in line with a 30-m accumulation of glaciogenic unit III northeast of the Vaygach Island, possibly representing a terminal morainic ridge (Fig. 7; V. Gataullin, pers. commun.). In this interpretation, unit III deposits west and east of the ice margin have different ages, like the lower part of unit II. Additional geological correlation is needed to verify this stratigraphy.

Although the position of the LGM margin in the Kara Sea east of the study area is mostly speculative (Fig. 7; Svendsen et al. 1999), there are clear maximum and minimum scenarios. Our minimal configura-

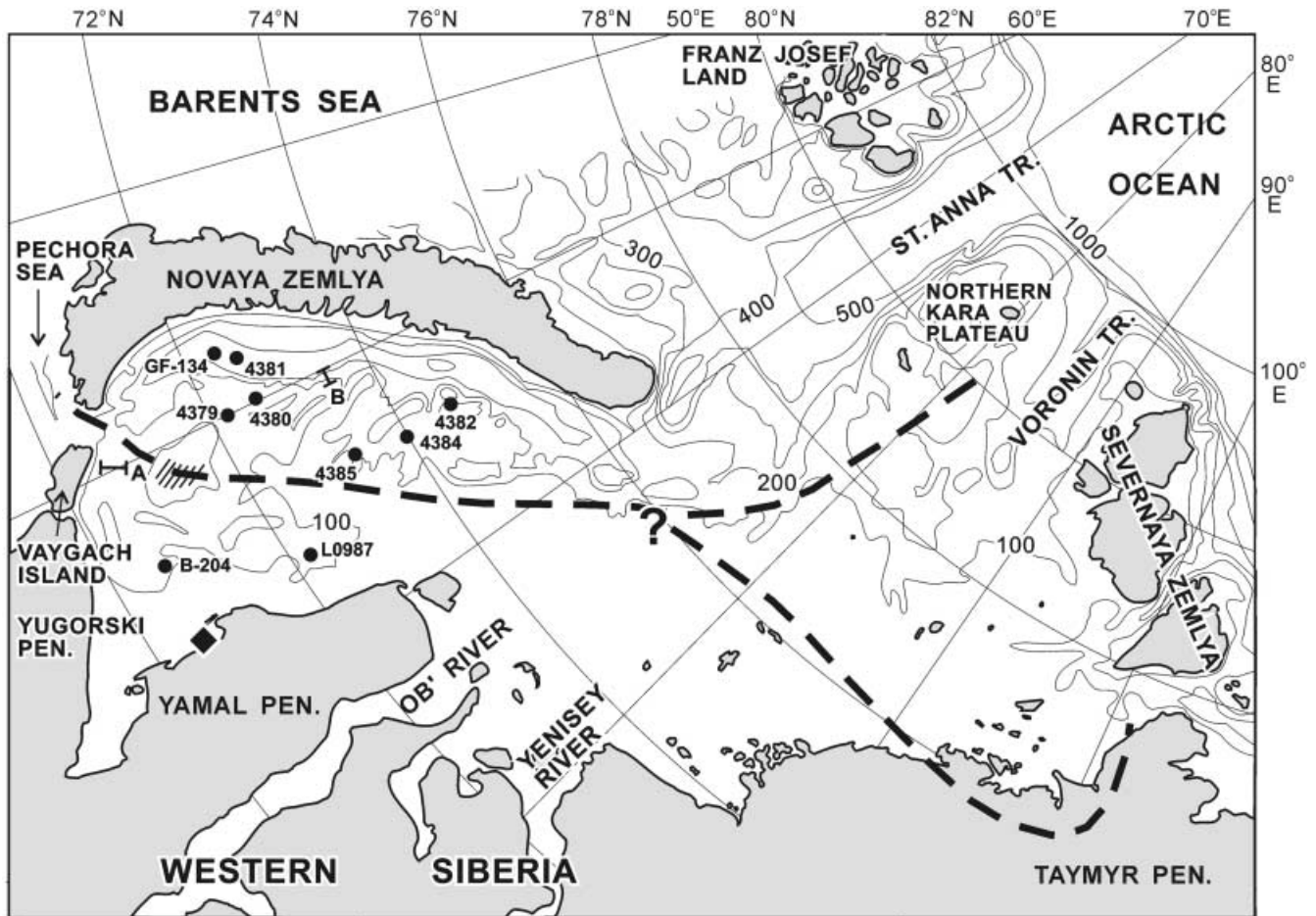


Fig. 7 Suggested scenarios for the LGM limit in the Kara Sea (*dashed lines*). Sediment cores and sparker lines in the southwestern Kara Sea are same as in Fig. 1. The *hatched area* east of Vaygach Island shows an accumulation of glaciogenic deposit interpreted as a morainic ridge (V. Gataullin, pers. commun.). The *diamond* shows the site at the Yamal coast that remained unglaciated since Middle/Early Weichselian time (Forman et al. 1999)

tion includes extension of the ice-sheet margin to the Northern Kara Plateau to account for the grounded ice in the Saint Anna Trough (Polyak et al. 1997a; Hald et al. 1999), but the eastern Kara Sea will remain unglaciated; however, the evidence for LGM ice impinging on the northwestern Taymyr Peninsula (Alexanderson et al. 2000) indicates the possibility that the Barents-Kara ice sheet extended across at least the northern Kara Sea. Solving the discrepancy between these two scenarios is crucial not only for the assessment of the LGM ice volume in the Eurasian Arctic, but also for understanding the history of the Ob' and Yenisey river discharge. In the minimum ice-sheet configuration, the voluminous flow of these rivers into the Arctic Ocean would be unconstrained during the Late Weichselian. In contrast, in the maximum scenario, they would be dammed by ice to form a proglacial lake on the Kara Sea shelf, similar to gigantic

paleo-lakes that likely formed on the Siberian lowlands during earlier glaciations (Arkhipov et al. 1995).

Conclusion

Seismo- and lithostratigraphic data indicate that the entire southwestern Kara Sea has been covered by a grounded ice sheet. However, the age of glaciogenic deposits may vary across the study area. The last glacial expansion overriding the Novaya Zemlya Trough likely occurred during the LGM, whereas the area further east may have remained unglaciated since Middle/Early Weichselian time. The minimum age of the last glacial retreat from the western area is constrained by a ^{14}C date of 11.8 ka and the complete deglaciation of the shelf occurred by ca. 10 ka. The northeastward extension of our inferred LGM margin from the southwestern Kara Sea has two possible scenarios: one involving an unglaciated eastern Kara Sea and the unhindered flow of the Ob' and Yenisey rivers into the Arctic Ocean; and another implying ice-sheet damming of rivers on the shelf.

Late Weichselian sedimentary environments in the southwestern Kara Sea east of the ice-sheet margin were characterized by a strong influence of river runoff, reflecting the extension of the Ob' and Yenisey

rivers on the shelf. The riverine signature in mineralogical, paleobiological, and geochemical proxies abruptly diminished with the sea-level rise by ca. 9 ka. Further changes in proxy records indicate less pronounced reorganizations in the hydrographic regime. A departure in stable-isotopic values between western and eastern parts of the study area at ca. 7 ka is interpreted to indicate the formation of fully saline deep water in the Novaya Zemlya Trough. Subsequent changes in sedimentary, foraminiferal, and stable-isotopic records presumably indicate the invigoration of surface-water circulation and/or reduction in riverine inputs in the southwestern Kara Sea between ca. 7 and 3 ka. Riverine inputs may have partially regained in the late Holocene, after ca. 3 ka, possibly in connection with the establishment of heavier sea-ice conditions.

Acknowledgements This is Byrd Polar Research Center Contribution no. 1184 supported by the NSF grants OPP-9529133 and OPP-9818247. Work of M. Levitan and T. Khusid was also supported by RFBR-CNRS grant 98-05-22029. We are grateful to all persons and institutions who have been involved in collecting and processing of materials used in the publication. Reviews by C. Hjort and M. Hald and comments by D.J. Lubinski helped improving the manuscript.

References

- Alexanderson H, Hjort C, Antonov O, Möller P, Pavlov M (2000) Landforms, sediments and age of the North Taymyr ice-marginal zone, Siberia. Abstract, 4th QUEEN Workshop, Lund, Sweden, 7–10 April, p 1
- Arkhipov SA, Isaeva LL, Besspalov VG and Glushkova OYu (1986) Glaciation of Siberia and northeast USSR. In: Sibrava V et al. (eds) Quaternary glaciations in the Northern Hemisphere. Pergamon Press, Oxford, pp 463–474
- Arkhipov SA, Ehlers J, Johnson RG, Wright HE Jr (1995) Glacial drainage towards the Mediterranean during the Middle and Late Pleistocene. *Boreas* 24:196–206
- Astakhov V (1992) The last glaciation in West Siberia. *Sveriges Geol Unders Ca* 81:21–30
- Behrends M (1999) Reconstruction of sea-ice drift and terrigenous sediment supply in the Late Quaternary: heavy-mineral associations in sediments of the Laptev-Sea continental margin and the central Arctic Ocean. *Ber Polarforsch* 310:1–167
- Dunaev NN, Levitan MA, Kuptsov VM (1996) Physical properties of Late Quaternary sediments within Kara shelf and conditions of their formation. *Oceanology (Russia)* 35:833–839
- Elverhøi A, Solheim A (1983) The Barents Sea ice sheet: a sedimentological discussion. *Polar Res* 1:23–42
- Erlenkeuser H, Spielhagen R, Taldenkova E (1999) Stable isotopes in modern water and bivalve samples from the southern Kara Sea. *Ber Polarforsch* 300:80–90
- Fairbanks RG (1989) A 17,000 year glacio-eustatic sea-level record: influence of glacial melting on the Younger Dryas event and deep-ocean circulation. *Nature* 342:637–642
- Forman SL, Lubinski D, Miller GH, Matishov G, Snyder J, Korsun S, Myslivets V (1995) Post-glacial emergence and distribution of Late Weichselian ice sheet loads in the northern Barents and Kara Seas, Russia. *Geology* 23:113–116
- Forman SL, Gataullin V, Ingólfsson O, Lokrantz H, Manley W (1999) Late Quaternary stratigraphy of western Yamal Peninsula, Russia: new constraints on the configuration of the Eurasian ice sheet. *Geology* 27:807–810
- Gataullin V, Polyak L (1997) Subglacial channels, southern Barents Sea. In: Davies TA, Bell T, Cooper AK, Josenhans H, Polyak L, Solheim A, Stoker MS, Stravers J (eds) *Glaciated continental margins: an atlas of acoustic images*. Chapman and Hall, London, pp 64–65
- Gataullin VN et al. (1992) Lithostratigraphic investigation of the key geotechnical boreholes in the Barents and Kara Sea. *Tech Rep Sojuzmorinzheologia*, Riga, 363 pp (in Russian)
- Gataullin VN, Polyak LV, Epstein OG, Romanyuk BF (1993) Glacigenic deposits of the Central Deep: a key to the Late Quaternary evolution of the eastern Barents Sea. *Boreas* 22:47–58
- Gataullin V, Mangerud J, Svendsen JI (in press) The Late Pleistocene glacial history of the Pechora (SE Barents) Sea: mapping results from the seismic reflection data. *Global Planet Change*
- Grosswald MG (1994) The drumlin fields of the Novaya Zemlya: Urals region and the Kara center of glaciation. *Polar Geogr Geol* 18:15–32
- Hahne J, Melles M (1999) Climate and vegetation history of the Taymyr Peninsula since Middle Weichselian time: palynological evidence from lake sediments. In: Kassens H, Bauch HA, Dmitrenko I, Eicken H, Hubberten HW, Melles M, Timokhov L (eds) *Land-ocean systems in the Siberian Arctic: dynamics and history*. Springer, Berlin Heidelberg New York, pp 407–423
- Hald M, Steinsund PI, Dokken T, Korsun S, Polyak L, Aspeli R (1994) Recent and Late Quaternary distribution of *Elphidium excavatum* f. *clavata* in Arctic seas. *Cushman Found Spec Publ* 32:141–153
- Hald M, Kolstad V, Polyak L, Forman SL, Herlihy FA, Ivanov G, Nescheretov A (1999) Late-glacial and Holocene paleoceanography and sedimentary environments in the St. Anna Trough, Eurasian Arctic Ocean. *Palaeogeogr Palaeoclimatol* 146:229–249
- Khusid TK, Korsun SA (1996) Modern benthic foraminiferal assemblages in the Kara Sea. *Ber Polarforsch* 212:308–314
- Krapivner RB, Gritzenko II, Kostyukhin AI (1988) The Late Cenozoic seismostratigraphy and paleogeography of the Southern Barents Sea region. In: Matishov GG, Tarasov GA (eds) *Quaternary paleoecology and paleogeography of the northern seas*. Nauka, Moscow, pp 103–123 (in Russian)
- Kulikov NN (1971) Mineral composition of the sand/silt fraction of the Kara Sea sediments. In: Lapina NN (ed) *Geologiya morya*. NIIGA, Leningrad, pp 64–72 (in Russian)
- Levitan MA, Khusid TA, Kuptsov VM, Politova NV, Pavlova GA (1995) Types of Upper Quaternary cross-sections in the Kara Sea. *Oceanology (Russia)* 34:710–721
- Levitan MA, Dekov VM, Gorbunova ZN, Gurvich EG, Muiakshin SI, Nurnberg D, Pavlidis MA, Ruskova NP, Shelekhova ES, Vasilkov AP, Wahsner M (1996) The Kara Sea: a reflection of modern environment in grain size, mineralogy and chemical composition of the surface layer of bottom sediments. *Ber Polarforsch* 212:58–81
- Lisitzin AP, Vinogradov ME (1995) International high-latitude expedition in the Kara Sea (the 49th cruise of the R/V *Dmitriy Mendeleev*). *Oceanology (Russia)* 34:583–590
- Lokrantz H, Ingólfsson Ó, Gataullin V (2000) Late Pleistocene stratigraphy and glaciodynamics at Cape Spindler, Yugorsky Peninsula, Arctic Russia. Abstract, 4th QUEEN Workshop, Lund, Sweden, 7–10 April, p 30
- Lubinski DJ, Korsun S, Polyak L, Forman SL, Lehman SJ, Herlihy FA, Miller GH (1996) The last deglaciation of the Franz Victoria Trough, northern Barents Sea. *Boreas* 25:89–100
- Mangerud J, Svendsen JI, Astakhov VI (1999) Age and extent of the Barents and Kara ice sheets in northern Russia. *Boreas* 28:46–80
- McCorkle DC, Keigwin LD, Corliss BH, Emerson SR (1990) The influence of microhabitats on the carbon isotopic composition of deep-sea benthic foraminifera. *Paleoceanography* 5:161–185

- Mukhina VV, Yushina IG (1999) Diatoms in bottom sediments of the Laptev and Kara seas. *Ber Polarforsch* 306:110–119
- Okulitch AV, Lopatin BG, Jackson HR (1989) Circumpolar geological map of the Arctic. *Geol Surv Can Map* 1765 A
- Polyak L, Mikhailov V (1996) Post-glacial environments of the southeastern Barents Sea: foraminiferal evidence. In: Andrews JT et al. (eds) *Late Quaternary paleoceanography of the North Atlantic margins*. *Geol Soc Spec Publ* 111:323–337
- Pavlov VK, Pfirman SL (1995) Hydrographic structure and variability of the Kara Sea: implications for pollutant distribution. *Deep-Sea Res II* 42:1369–1390
- Polyak L, Solheim A (1994) Late- and post-glacial environments in the northern Barents Sea west of Franz Josef Land. *Polar Res* 13:197–207
- Polyak L, Lehman SJ, Gataullin V, Jull AJT (1995) Two-step deglaciation of the southeastern Barents Sea. *Geology* 23:567–571
- Polyak L, Forman SL, Herlihy FA, Ivanov G, Krinitsky P (1997a) Late Weichselian deglacial history of the Svyataya (Saint) Anna Trough, northern Kara Sea, Arctic Russia. *Mar Geol* 143:169–188
- Polyak L, Khusid T, Stanovoy V (1997b) Benthic foraminifers as environmental indicators in the southern Kara Sea, Russian Arctic. Abstract, Application of micropaleontology in environmental sciences, 1st Int Conf, Tel Aviv, Israel, 15–20 June, pp 99–100
- Polyak L, Gataullin V, Epshtein O, Okuneva O, Stelle V (2000) New constraints on the limits of the Barents-Kara Ice Sheet during the Last Glacial Maximum based on borehole stratigraphy from the Pechora Sea. *Geology* 28:611–614
- Sættem J, Poole DAR, Ellingsen KL, Sejrup HP (1992) Glacial geology of outer Bjørnøya, southwestern Barents Sea. *Mar Geol* 103:15–51
- Serebryanny L, Andreev A, Malyasova E, Tarasov P, Romanenko F (1998) Late-glacial and early-Holocene environments of Novaya Zemlya and the Kara Sea region of the Russian Arctic. *Holocene* 8:323–330
- Sohlenius G (1996) Mineral magnetic properties of Late Weichselian – Holocene sediments from the northwestern Baltic Proper. *Boreas* 25:79–88
- Solheim A, Kristoffersen Y (1984) The physical environment, western Barents Sea. Sediments above the Upper Regional Unconformity: thickness, seismic stratigraphy and outline of the glacial history. *Norwegian Polarinst Skr* 179 B:1–26
- Solheim A, Russwurm L, Elverhøy A, Nyland-Berg M (1990) Glacial geomorphic features in the northern Barents Sea: direct evidence for grounded ice and implications for the pattern of deglaciation and late glacial sedimentation. In: Dowdeswell JA, Scourse JD (eds) *Glaciomarine environments: processes and sediments*. *Geol Soc Spec Publ* 53:253–268
- Spesivtsev VI et al. (1986) Geotechnical studies on the shelf of the Kara Sea (Leningrad structure). *Tech Rep AMIGE, Murmansk, Russia* (in Russian)
- Stuiver M, Braziunas T (1993) Modelling atmospheric ^{14}C influences and ^{14}C ages of marine samples to 10,000 BC. *Radiocarbon* 35:137–189
- Svendsen JI, Astakhov VI, Bolshiyakov DY, Demidov I, Dowdeswell JA, Gataullin V, Hjort C, Hubberten HW, Larsen E, Mangerud J, Melles M, Möller P, Saarnisto M, Siegert MJ (1999) Maximum extent of the Eurasian ice sheets in the Barents and Kara Sea region during the Weichselian. *Boreas* 28:234–242
- Valpeter AP et al. (1985) Investigation of geotechnical conditions of some oil and gas prone areas of the Kara Sea. *Tech Rep, Sojuzmorinzgeologia, Riga*, 500 pp (in Russian)
- Vedernikov VI, Demidov AB, AI Sudbin (1994) Primary production and chlorophyll in the Kara Sea in September 1993. *Oceanology (Russia)* 34:693–703
- Yashin DS, Mel'nitsky VYe, Kirillov OV (1985) Structure and composition of bottom deposits of the Barents Sea. In: Verba ML (ed) *Geological structure of the Barents and Kara Sea shelf*. *Sevmorgeologia, Leningrad*, pp 101–115 (in Russian)